Permanent Deformation on Preexisting Sliding Surfaces in Dams

By George Gazetas,[1] Member, ASCE, and Nasim Uddin[2]

Abstract: A finite-element model capable of computing permanent deformations along preexisting sliding surfaces in dams and embankments is used to evaluate the error in the current state-of-practice two-step procedures that are based on the simplifying assumption that the computation of dynamic response and of the resulting sliding displacements can be decoupled. Both sinusoidal and real earthquake ground motions are used as excitation, and Coulomb's friction law governs sliding along any point of the rigid-plastic tensionless interface. It is found that only when the dominant excitation frequencies lie in the proximity of the fundamental dam frequency will the permanent deformation from the decoupling assumption exceed appreciably the "single-step" value. As a validation of the single-step procedure, an analysis is performed and shown to successfully explain the nonsymmetric response of La Villita Dam recorded in the 1985 Mexico Earthquake.

INTRODUCTION

Newmark (1965) deduced that earth slopes do not necessarily fail just because the transient factor of safety against wedge sliding reaches (momentarily) a value below unity. Instead, permanent deformations of only a limited magnitude take place, as the direction of the "driving" acceleration quickly reverses and the sliding of the soil wedge stops.

Seed and Martin (1966), Ambraseys and Sarma (1967), and Makdisi and Seed (1978), applying Newmark's sliding-block concept, developed simplified procedures for predicting the permanent displacements of dams subjected to earthquake shaking. The magnitude of such displacements has since been introduced in safety performance criteria, in place of the "factor of safety" against limit-equilibrium failure (Marcuson et al. 1992). In its complete form, this simplified procedure includes for any trial failure surface two steps [Fig. 1(*b*)]:

1. Perform a dynamic analysis of the dam assuming that no failure surfaces exist. Determine the time history of acceleration at a number of locations within a hypothetical potentially sliding wedge, and at each instant of time average the accelerations over the whole volume of this wedge. The result is the (spatially) average time history of acceleration for the soil above the hypothetical failure surface.
2. Use this average time history of acceleration as the "driving" support motion in a sliding-block analysis, where the mass of the block equals the mass of the wedge, and set the horizontal force required to initiate sliding equal to the horizontal yield acceleration (pseudostatically determined) of the wedge. Compute the resulting permanent slip along the sliding interface.

[1]Prof. of Civ. Engrg., National Tech. Univ., Athens, Greece, and State Univ. of New York, Buffalo, N.Y., 14260.

[2]Engr., Acres Int., Corp., Amherst, N.Y., 14228-1180; formerly Grad. Student, Civ. Engrg., State Univ. of New York, Buffalo, N.Y.

Note. Discussion open until April 1, 1995. To extend the closing date one month, a written request must be filed with the ASCE Manager of Journals. The manuscript for this paper was submitted for review and possible publication on December 7, 1993. This paper is part of the ***Journal of Geotechnical Engineering***, Vol. 120, No. 11, November, 1994. ©ASCE, ISSN 0733-9410/94/0011-2041/$2.00 + $.25 per page. Paper No. 7433.

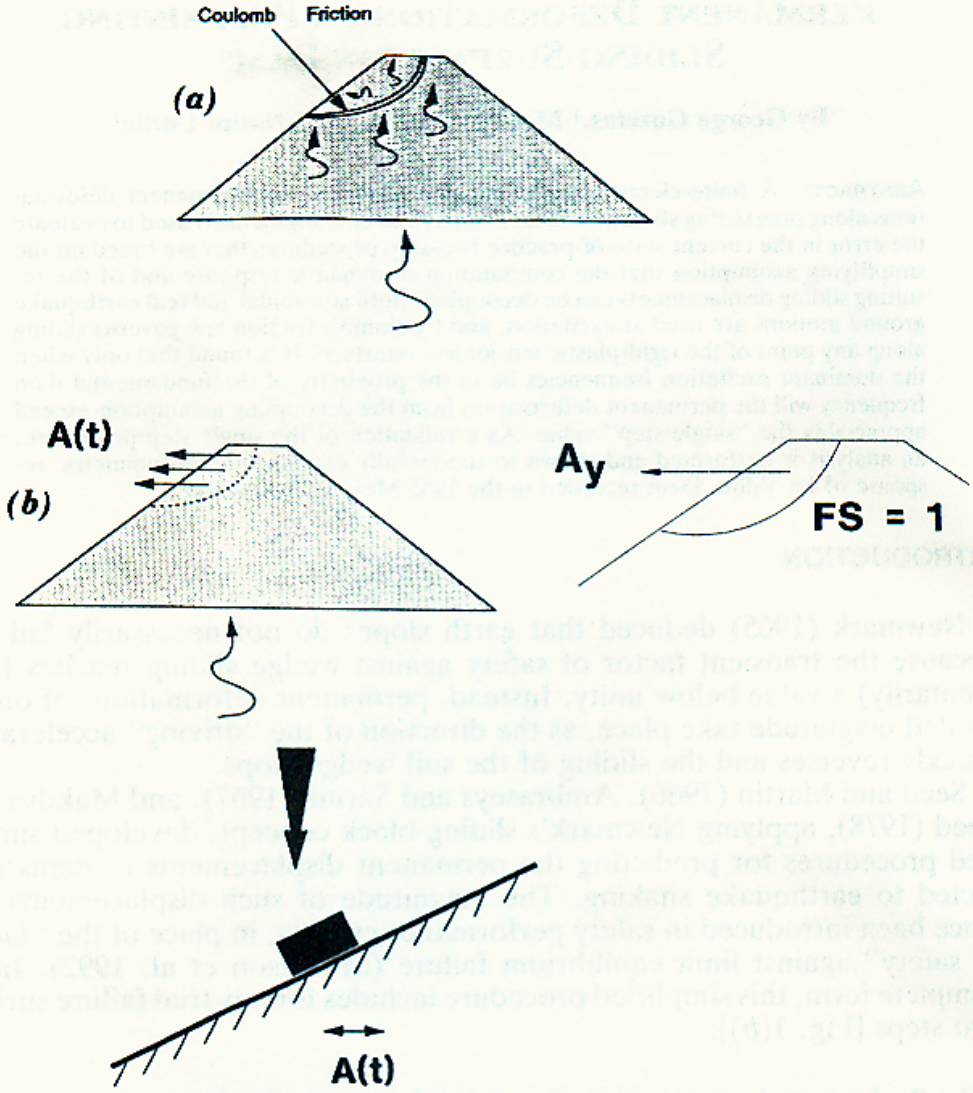

FIG. 1. Analyses: (*a*) Single-Step (PEPSI) Analysis: Dynamic Response with Simultaneous Sliding along PEPSI; and (*b*) Two-Step (Decoupled) Analysis: Top—Dynamic Response of Intact Dam and Pseudostatic Yield Acceleration; Bottom—Sliding of Rigid Block in Interface Failing at $A > A_y$

This simplified two-step procedure (which is hereafter also called the decoupled method) is based on three key assumptions:

- Computation of the elastic dynamic response and of the inelastic plastic slip can be decoupled and carried out separately.
- All permanent deformation occurs in concentrated fashion along the slip surface.
- The sliding block behaves like a rigid body.

Although intuitively logical, these simplifying assumptions have been tested only indirectly. For example, Lin and Whitman (1983) evaluated the error introduced by the decoupling assumption using simple lumped-parameter shear-beam type oscillators to model a typical earth dam. They found the method to be acceptable within certain limits.

On the other hand, several studies have been concerned with the uncer-

tainties in the computed sliding displacements stemming from different amplitudes and frequency characteristics, and even the details of the driving ground accelerations. Such studies have resulted in improved computational tools, but always within the framework of the aforementioned two-step procedure (Sarma 1975; Franklin and Chang 1977; Constantinou et al. 1984a, 1984b; Hynes-Griffin and Franklin 1984; Lin and Whitman 1986; Yegian et al. 1991; Yan 1991). A comprehensive review was presented recently by Marcuson et al. (1992).

One main objective of the present paper is to investigate the validity of the two-step procedures, by assessing the effect of the presence of a sliding interface on the acceleration response of the dam.

Moreover, in many cases, zones or surfaces of weakness were found to have formed in dams after earthquake shocks or after other causes of distress; the response of the earth structures containing such a discontinuity is of interest. As an example, the 1985 Mexico Earthquake produced sliding movement in La Villita Dam, along an apparently preexisting failure surface. This earth-core rockfill dam was instrumented with a strong-motion accelerograph located in a part of the dam that, in all evidence, slipped repeatedly during past earthquakes. Elgamal et al. (1990) recently studied the records of this dam and compared them with results from sliding-block shaking tests. Such case histories can be supplemented by a limited body of data from centrifuge tests [e.g., Kutter (1982)].

Another example of preexisting potentially sliding surfaces is earth structures containing inclined geomembranes and geotextiles for a variety of purposes, where the geomembrane may act as a weak surface during seismic shaking. Yegian and Lahlaf (1992), studying such systems in the shaking table, observed that under dynamic excitation the shear stress transmitted from a geomembrane to a geotextile is small; when exceeded, relative displacements occur along the geomembrane-geotextile interface and accumulate in accord with the Newmark sliding-block model. Hence, concern about the dynamic response of a geotechnical facility, such as a landfill containing geosynthetics, should primarily be associated with the permanent relative displacement that may accumulate along the interface between the two geosynthetics.

Attempting to provide an improved understanding of the mechanism of the sliding deformations in earth dams, the present paper provides results with a more general "single-step" procedure to estimate the earthquake-induced permanent displacements, and examines the likely error introduced by the two-step procedures. A finite-element formulation that can implement Coulomb's friction law along a sliding tensionless interface is used to this end. Note that a similar type of analysis was advocated for gravity retaining walls by Nadim and Whitman (1983), who determined the permanent seismic displacements after assuming the presence of a predefined Coulomb-type sliding surface in the backfill.

CALCULATION OF PERMANENT DISPLACEMENT

Single-Step Solution

A two-dimensional plane-strain finite-element model for computing permanent displacements assuming a pre-existing potentionally sliding interface (PEPSI) whose location is fixed (but varied parametrically) is used in the present study. It is assumed that all irreversible shear distortion occurs in this sliding interface, the behavior of which is ideally rigid-plastic, obeying Coulomb's friction law. The two parts of the dam (above and below this

surface) remain equivalently linear viscoelastic, and their contact is assumed tensionless. To model the slip (and, perhaps, even separation) at the interface during the strong earthquake shaking, ADINA uses special interface elements. The procedure it follows is an iterative one: any segment of the interface would experience sliding if the ratio of the computed tangential to the normal forces were to exceed the local coefficient of friction. The tangential force is then updated to equal the local frictional capacity. Implementation of this assumption requires a fine enough finite-element discretization and relatively small time steps during the solution. This single-step finite-element procedure, although also an approximation to reality, improves over the two-step method in that

- It accounts for changes in the dynamic response (intensity and frequency content) due to the presence of the failure surface (reflection and refraction of waves).
- The sliding mass as well as the underlying dam retain their elasticity during sliding (being flexible rather than rigid bodies).

On the other hand, this single-step method is an expensive alternative for routine computations.

Two-Step (Decoupled) Solution

During the first stage of this method, analysis is performed ignoring the (potential or actual) presence of the sliding surface (i.e., considering an intact dam). The average acceleration history of all nodal points in the sliding wedge and pseudostatic horizontal yield acceleration are then evaluated and used in Newmark-type sliding-block analysis, as already explained.

GEOMETRY AND MATERIALS OF STUDIED DAM

A typical 100-m-tall rockfill dam, is studied herein to compare the response computed using the decoupling assumption with that calculated by a single-step procedure. The dam is symmetric with 1.5H:1V slopes and a 10-m-wide crest.

The dynamic behavior of rockfill is described through: (1) The small-strain shear modulus G_{max}; (2) the decrease of secant modulus G with increasing strain γ; (3) the hysteretic damping ratio β, which is an increasing function of the amplitude of shear strain γ; and (4) the Poisson's ratio ν. Published experimental results from the literature were used to assign realistic values to the material parameters (Seed et al. 1986). Thus, the spatial distribution of G_{max} was estimated as a function of the effective confining pressure, $\sigma_m = (\sigma_1 + \sigma_2 + \sigma_3)/3$, of each rockfill element

$$G_{max} = 1{,}000(K_{2max})(\sigma_m)^{1/2} \quad (1)$$

where K_{2max} has units of square root of stress, and its value for compacted gravels and rockfill is in the range of 150–250 if stresses are in lb/ft^2 (or about 40–70 if stresses are in kPa). Back analysis by Mejia et al. (1982) of the response of the Orovile Dam (California) to a weak seismic shaking gave $K_{2max} = 170$. In our study K_{2max} was varied parametrically between 150 and 250, if only to confirm that the conclusions regarding the performance of the dam are not sensitive to the exact value of this parameter. Static analyses were first carried out using the finite-element code ADINA

(Bathe et al. 1988), to obtain the effective mean principal stress σ_m in all elements.

Poisson's ratio ν for dry or nearly dry rockfill is taken equal to 0.25. Note that while ν has only a marginal influence on lateral oscillations, it may play an appreciable role in rocking-type, longitudinal, and especially vertical oscillations (e.g., Gazetas 1981a, 1981b).

Some limited data is available for estimating the decline of secant shear modulus G with increasing γ in rockfill; they reveal a slightly faster rate of decline than for clayey soils. On the other hand, the data for the dependence of β on γ show a slightly faster rate of increase than for sands and clays (Seed et al. 1986).

Having modeled the plane geometry and dynamic properties of the dam, iterative two-dimensional "equivalent linear" viscoelastic analyses were performed in which the shear modulus G and damping ratio β were obtained from the "effective" shear strain level of the previous iteration. The effective shear strain was obtained as the two-thirds fraction of the peak value. All analyses were performed with ADINA, (Bathe et al. 1988), which uses Newmark's time-integration algorithm for a direct step-by-step solution.

RESULTS USING SINUSOIDAL GROUND MOTION

Fig. 2 sketches the studied rockfill dam. Two different models were used, corresponding roughly to the cases of shallow and deep failure wedges in the dam (interface 1 and interface 2, respectively), as indicated by the finite-element meshes in the figure. Using the properties discussed in previous sections, the response of the dam is first analyzed in this section using as input a simple sinusoidal ground motion with five pulses of acceleration. (This was done to study some details of response that may be obscured by the erratic nature of an actual ground motion.)

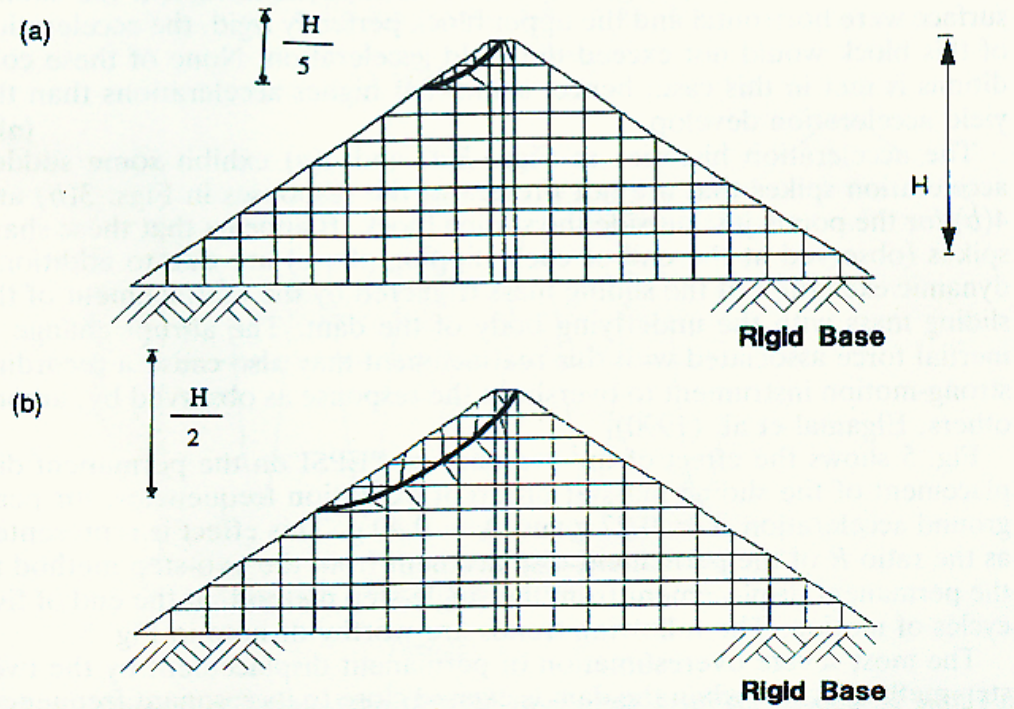

FIG. 2. Mesh with PEPSI of Yield Acceleration: (a) $A_y \approx 0.30$ g (Interface 1); and (b) $A_y \approx 0.50$ g (Interface 2)

The "yield" accelerations A_y of the sliding interfaces (PEPSI) 1 and 2 were statically determined for a friction angle of 45° to equal about 0.30 g and 0.50 g, respectively. Ground-acceleration amplitudes of $A = 0.27$ g and 0.4 g along with several different values of the frequency ratios f/f_1, where f is the excitation frequency and f_1 is the fundamental frequency of the dam, were applied. Twenty interface elements model the sliding interface. Nonlinearities may thus occur in only 20 elements of the finite-element assemblage.

Figs. 3 and 4 show some details of typical results using the single-step method, at a frequency ratio $f/f_1 = 0.75$ and ground acceleration $A = 0.40$ g. Figs. 3(a) and 4(a) portray the acceleration histories of two points inside the sliding block, and Figs. 3(b) and 4(b) portray the histories of two points just outside the sliding block for the dam with PEPSI No. 2. First we note that the time histories in Figs. 3(b) and 4(b) are rather similar to those derived for the intact dam, without a sliding interface [Fig. 3(c)]. However, some high-frequency spikes are generated during the half-cycles where the wedge tends to move inward relative to the supporting dam ("sticking" phase). Similar spikes have been observed in other studies of sliding systems (Ambraseys 1973; Makris 1989; and Succarieh 1990).

On the other hand, the acceleration histories of the points inside the PEPSI [Figs. 3(a) and 4(a)] consistently exhibit an asymmetric pattern that is comparable to the acceleration response of a block sliding on an inclined plane. During the sticking phase, the absolute acceleration of the sliding mass is the same as that of the dam. During slippage, however, the absolute acceleration of the sliding mass deviates from that of the dam. A peak acceleration of roughly constant amplitude is maintained during the slip phase. Apparently, this asymmetry between negative and positive peak values of acceleration is due to the "truncation" of the positive peaks because of the slippage. The inertia force that can be transmitted to the sliding mass is limited by the wedge's "yield" acceleration. In fact, if the sliding surface were horizontal and the upper block perfectly rigid, the acceleration of this block would not exceed the yield acceleration. None of these conditions is met in this case; hence, somewhat higher accelerations than the yield acceleration develop.

The acceleration histories in Figs. 3(a) and 4(a) exhibit some sudden acceleration spikes that are not present at the responses in Figs. 3(b) and 4(b) for the points just outside the sliding block. It appears that these sharp spikes (observed at the end of each slipping phase) are due to additional dynamic excitation of the sliding mass triggered by the reattachment of the sliding mass with the underlying body of the dam. The abrupt change in inertial force associated with this reattachment may also cause a recording strong-motion instrument to overshoot the response as observed by, among others, Elgamal et al. (1990).

Fig. 5 shows the effect of the presence of PEPSI on the permanent displacement of the sliding mass at different excitation frequencies, for peak ground acceleration $A = 0.27$ g and $A = 0.40$ g. This effect is represented as the ratio R of the permanent displacement from the two-step method to the permanent displacement from the single-step method, at the end of five cycles of motion. The following trends are worthy of note in Fig. 5.

The most severe overestimation of permanent displacement by the two-step method occurs when the dam is excited close to its resonant frequency. This may be explained by the fact that in the single-step method, build-up of the response is drastically limited by the shearing strength of the inter-

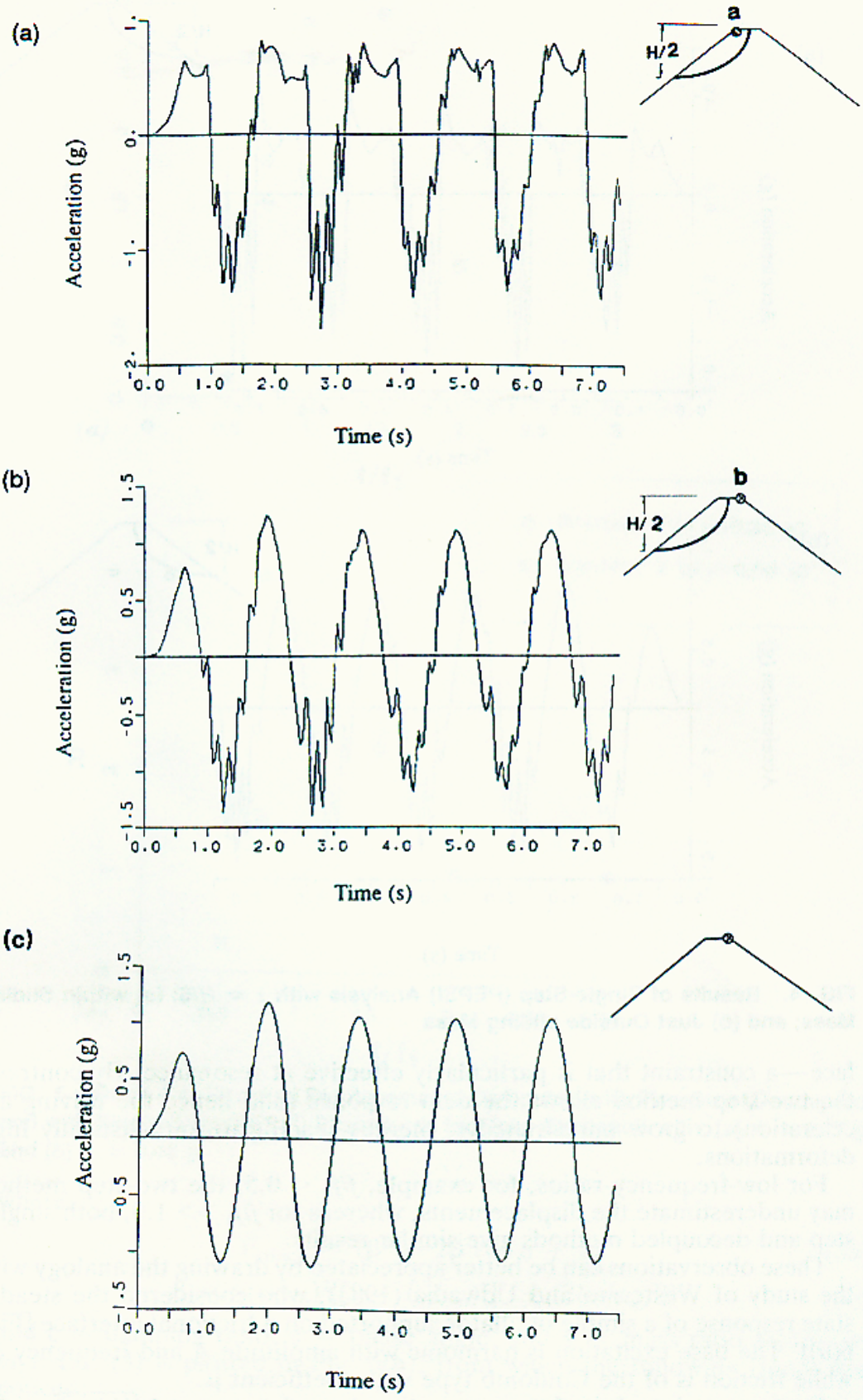

FIG. 3. Results of Single-Step (PEPSI) Response Analysis Compared with Response of Intact Dam (Crest $z = 0$): (*a*) within Sliding Mass; (*b*) Just Outside Sliding Mass; and (for Comparison) (*c*) Crest Acceleration of Intact Dam at Point b

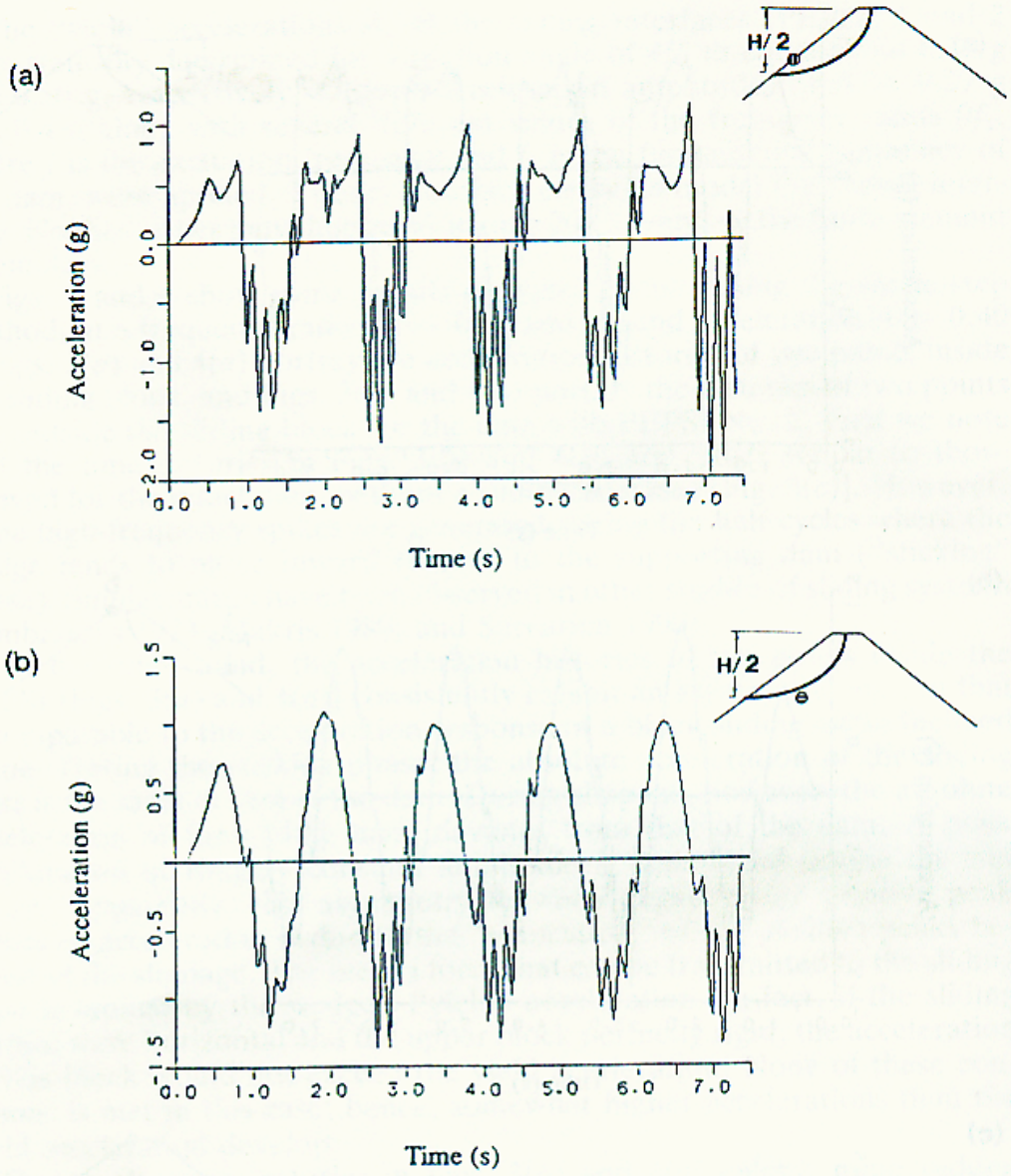

FIG. 4. Results of Single-Step (PEPSI) Analysis with $z = H/5$: (*a*) within Sliding Mass; and (*b*) Just Outside sliding Mass

face—a constraint that is particularly effective at resonance. By contrast, the two-step method allows the dam response (and hence the driving acceleration) to grow unrestrictedly, thereby leading to unrealistically high deformations.

For low-frequency ratios, for example, $f/f_1 < 0.5$, the two-step method may underestimate the displacements, whereas for $f/f_1 >> 1.0$, both single-step and decoupled methods give similar results.

These observations can be better appreciated by drawing the analogy with the study of Westermo and Udwadia (1983), who considered the steady-state response of a simple oscillator supported on a frictional interface [Fig. 6(*a*)]. The base excitation is harmonic with amplitude A and frequency ω, while friction is of the Coulomb type with coefficient μ.

For every value of the frequency ratio ω/ω_n, where $\omega_n = \sqrt{(k/m_1)}$ = the natural frequency of the fixed-base oscillator, slippage occurs whenever

$$F = \mu g/A \leq F_{\text{critical}} \tag{2}$$

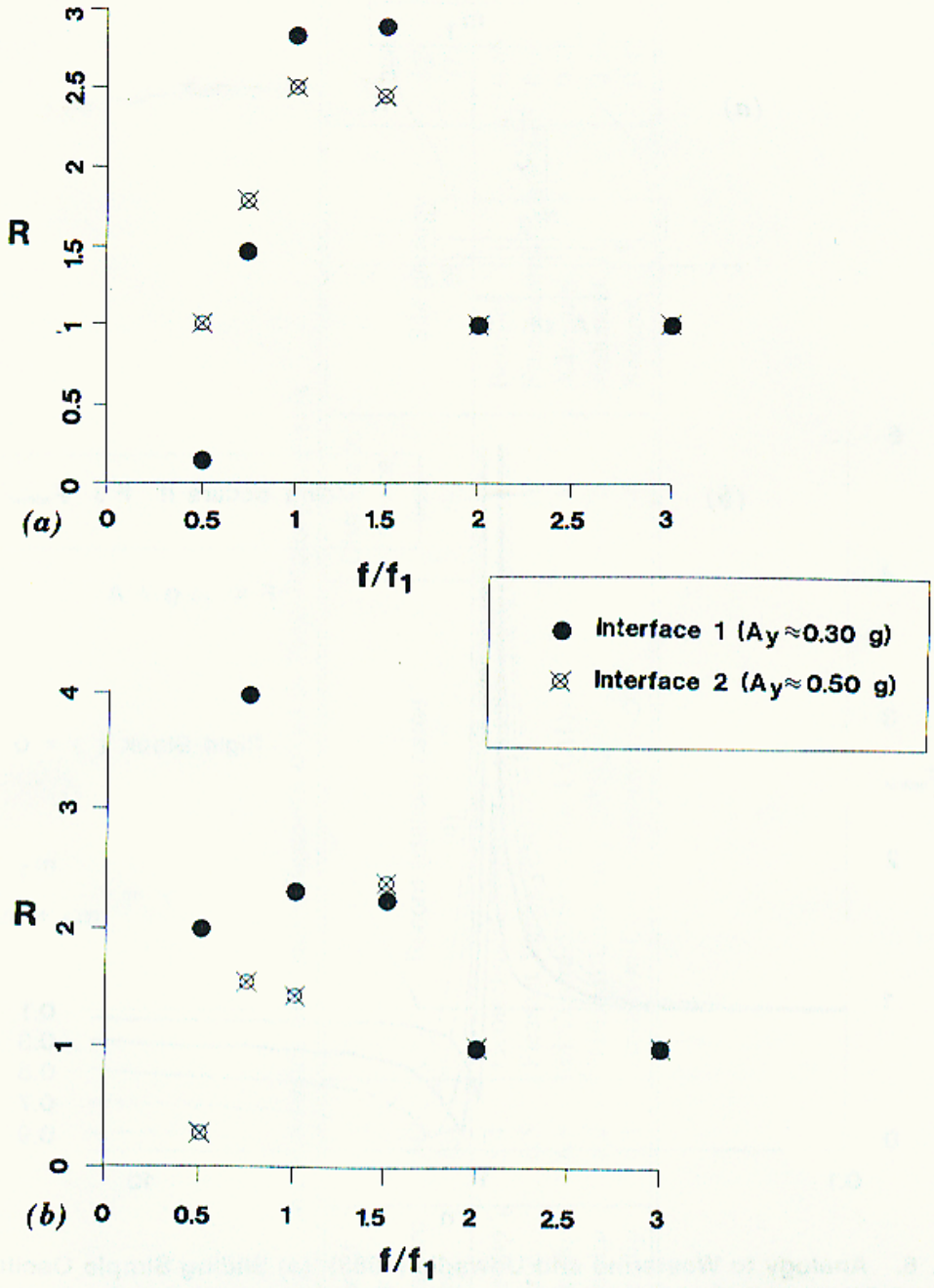

FIG. 5. Ratio R of Residual Displacements Computed with Two-Step (Decoupled) and with Single-Step (PEPSI) Procedures for Base Excitation with: (a) $A = 0.27$ g; and (b) $A = 0.40$ g

where

$$F_{\text{critical}} = (\beta^2 + 2\beta \cos\theta + 1)^{1/2} \tag{3a}$$

$$\beta = \gamma(\omega/\omega_n)^2\{[1 - (\omega/\omega_n)^2]^2 + (2\zeta\omega/\omega_n)^2\}^{1/2} \tag{3b}$$

and ζ = damping ratio; θ = phase angle; and γ = mass ratio $m_1/(m_1 + m_2)$. Eq. (3) is plotted in Fig. 6(*b*), from which the following trends are noticed:

- Slippage of a rigid block ($\omega_n \to \infty$) initiates whenever $F < 1$ or $A > \mu g$, as of course expected.

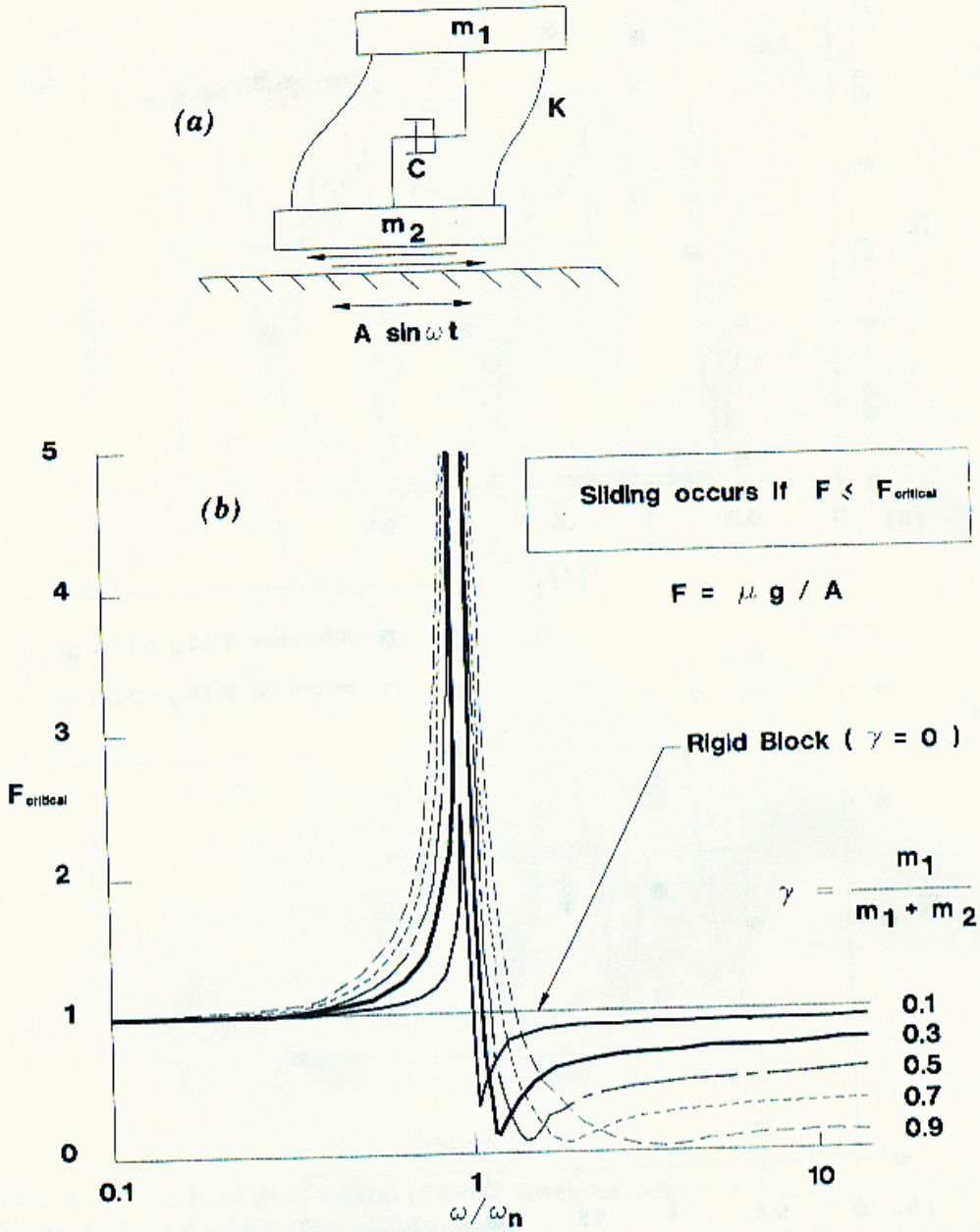

FIG. 6. Analogy to Westermo and Udwadia (1983): (a) Sliding Simple Oscillator; and (b) Effect of Ratio of Excitation Frequency to Natural Frequency on Critical Value of F ($=\mu g/A$) Required to Initiate Sliding of Oscillator

- Slippage of a flexible oscillator, on the other hand, initiates at higher values of F (and therefore lower values of A) if $\omega/\omega_n \approx 1$, and at lower values of F (higher value of A) if $\omega/\omega_n >> 1$. This is because at $\omega/\omega_n \approx 1$ the shear force exerted on mass m_2 from the oscillating mass m_1 is much larger than the inertia force $m_2\ddot{u}$ that m_2 would have experienced if no sliding took place. Hence, sliding is sustained primarily by the resonant oscillation of mass m_1. Basically, then, during the transient part of the motion, energy builds up in the oscillator, and at the steady state, the input energy balances the energy dissipated in frictional slippage and by viscous structural damping.

TABLE 1. Characteristics of Historic Records Used in Time-History Analysis

Earthquake name (1)	Style of rupture mechanism (2)	M_s (3)	Record (station) name (4)	Distance to source (km) (5)	Site geology (6)	pga (g) (7)
San Salvador (October, 1986)	Strike-slip	5.4	Geotechnical Investigation Center (GIC)	4	Bedrock	0.69
Coalinga (May, 1983)	Reverse	6.5	Pleasant Valley (PV)	11	Franciscan formation	0.60
Imperial Valley (October, 1979)	Strike-slip	6.9	El Centro Station NO. 1 (A1)	8	Alluvium	0.37
Nicaragua (March, 1973)	Strike-slip	6.2	National University (NU)	6	Sediment	0.36
Morgan Hill (April, 1984)	Strike-slip	6.1	Anderson Dam Abutment (AD)	4	Bedrock	0.42

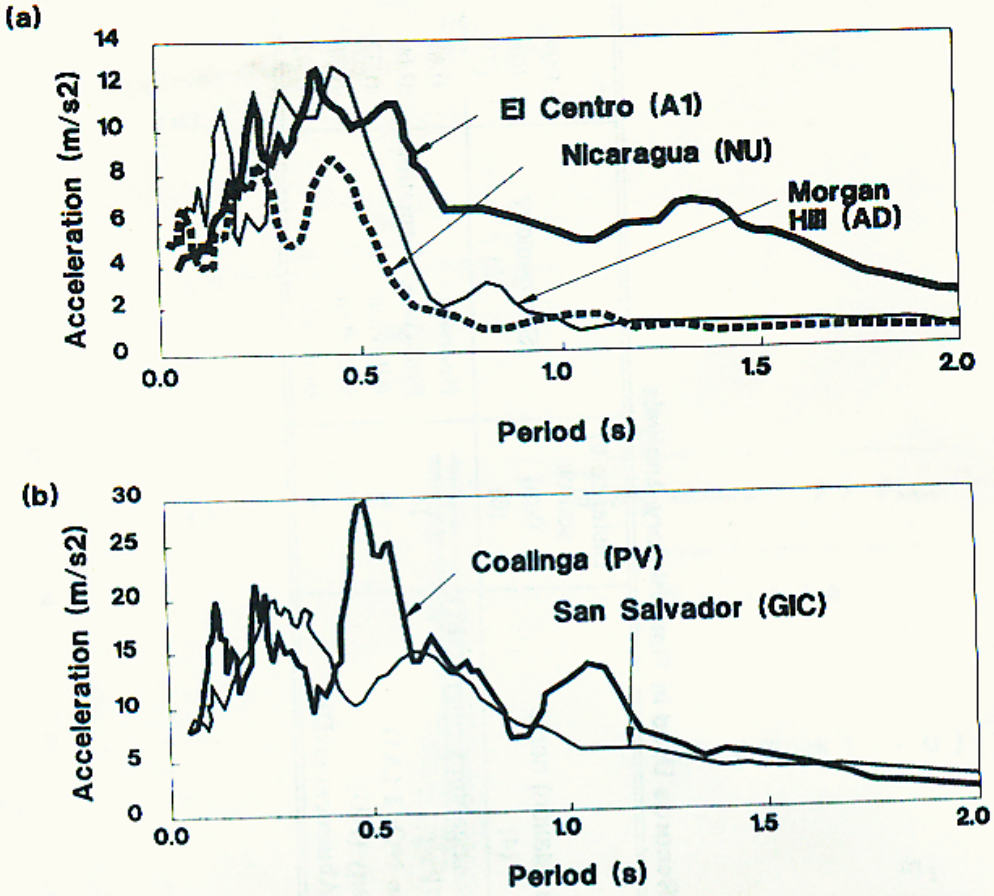

FIG. 7. Response Spectra of: (*a*) Moderately Strong Earthquake Records (pga ≈ 0.40 g); and (*b*) Very Strong Earthquake Records (pga ≈ 0.60–0.70 g) Used as Excitation

TABLE 2. Permanent Displacement (m) Calculated for Two Wedges (Interfaces 1 and 2) with Single-Step and Two-Step Methods

Earthquake/record (1)	Interface No. 1		Interface No. 2	
	Single-step (2)	Two-step (3)	Single-step (4)	Two-step (5)
San Salvador (1986)/GIC	0.55	0.50	0.18	0.18
Coalinga (1983)/PV	0.75	1.15	0.30	0.55
Imperial Valley (1979)/A1	0.50	0.49	0.12	0.18
Nicaragua (1973)/NU	0.01	0.02	0.00	0.00
Morgan Hill (1984)/AD	0.02	0.05	0.01	0.00

When $\omega/\omega_n > 1$, m_1 moves 180°, out of phase, with the excitation and with m_2 (at least when there is no sliding). Therefore, the oscillation of m_1 acts in a stabilizing way and reduces the extent of sliding for a given acceleration level. Hence, the acceleration A needed to initiate sliding is larger than for a rigid block of mass $m_1 + m_2$.

RESULTS FOR HISTORIC EARTHQUAKE RECORDS

In this section, accelerograms recorded in five historic earthquakes are usd as base excitation. Information on the records and the earthquake events

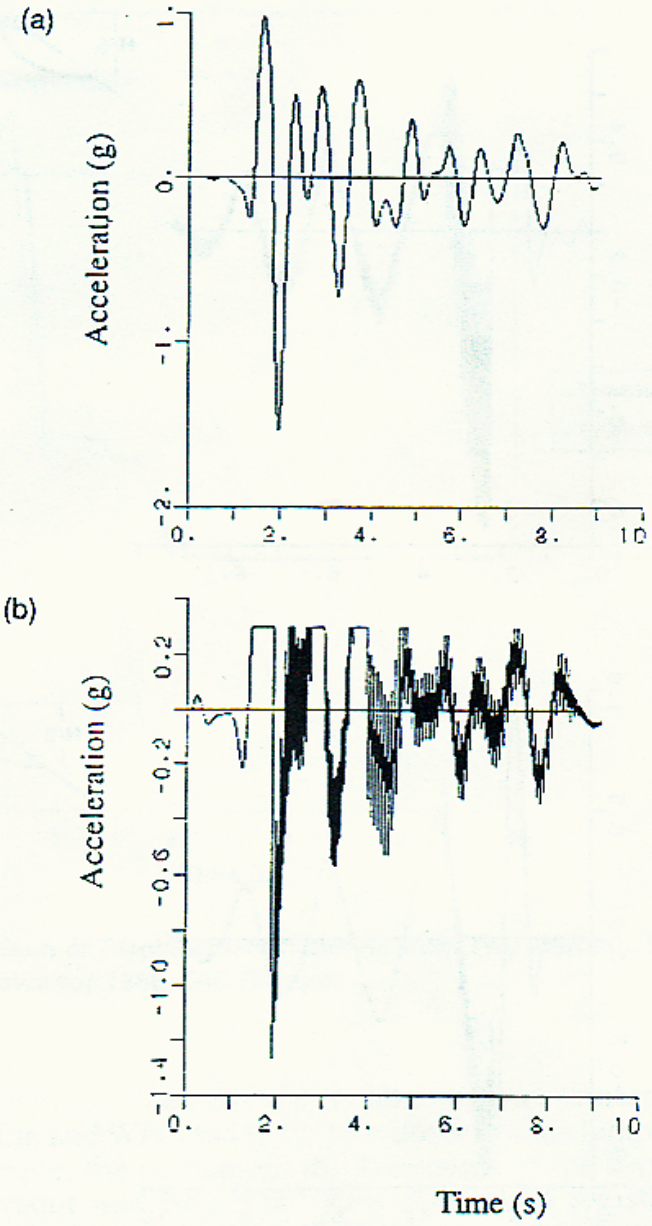

FIG. 8. Two-Step (Decoupled) Analysis (Wedge above Interface 1) for Acceleration Histories with Very Strong Excitation (San Salvador 1986, GIC): (*a*) Average "Driving" Acceleration; and (*b*) Sliding-Block Acceleration

are summarized in Table 1 and their response spectra are shown in Fig. 7. Based on the peak ground acceleration (pga) and distance from the source, these five records are divided into two groups: (1) Very strong motions (pga ≥ 0.60 g), which include records from the 1986 San Salvador [Geotechnical Information Center (GIC)] and the 1983 Coalinga [Pleasant Valley (PV)] earthquakes; and (2) moderately strong motions (pga ≈ 0.40 g), which include data from the 1979 Imperial Valley (El Centro A1), the 1973 Nicaragua [National University (NV)], and the 1984 Morgan Hill [Anderson Abutment Dam (AD)] earthquakes.

Typical results using the two-step and single-step procedures are summarized in Table 2 and presented graphically for the San Salvador record only [see Uddin (1992) for detailed results]. Figs. 8 and 9 show the typical

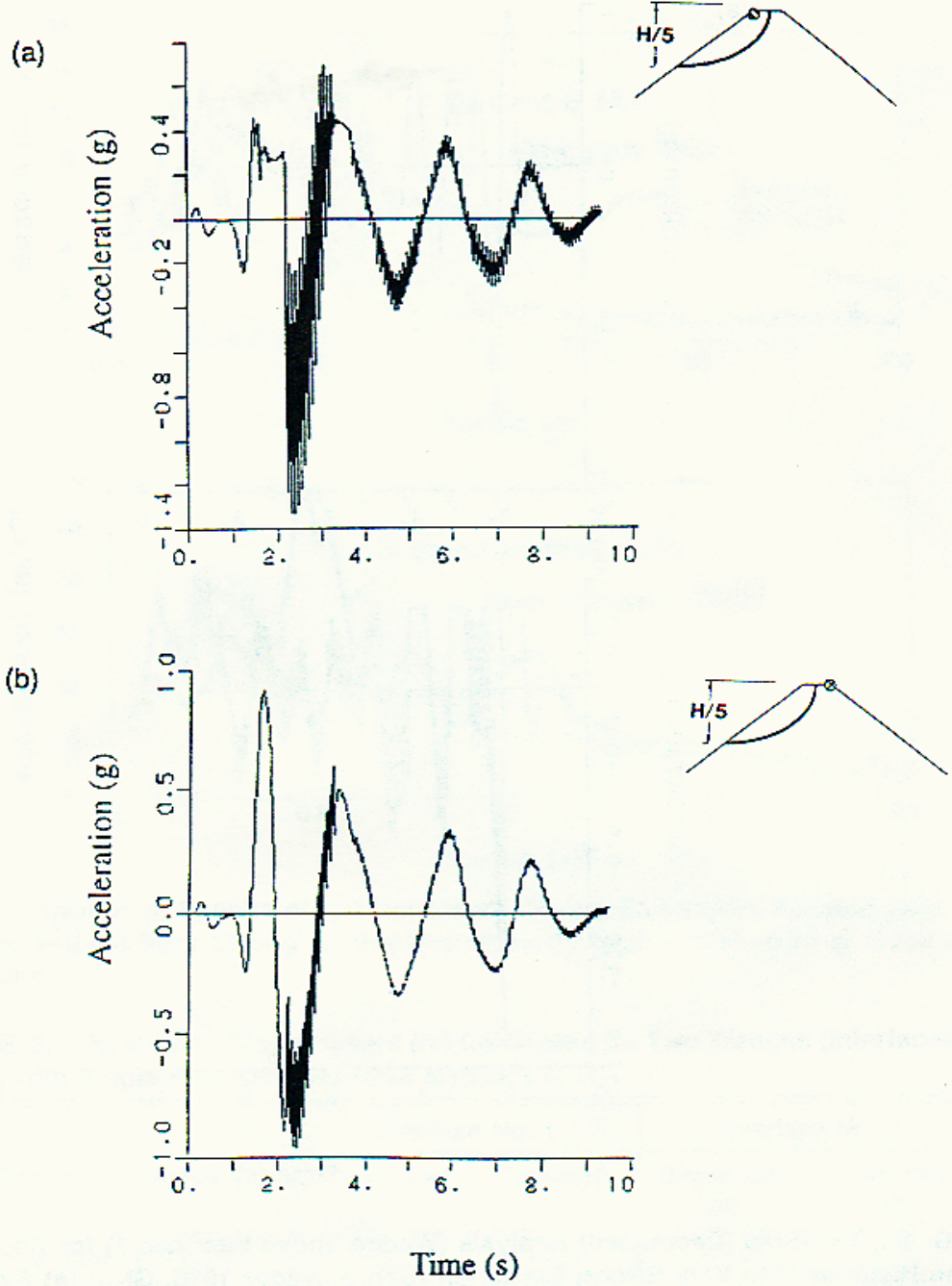

FIG. 9. Single-Step (PEPSI) Analysis (Wedge above Interface 1) for Acceleration Histories with Very Strong Excitation (San Salvador 1986, GIC): (*a*) within Sliding Mass; and (*b*) Just Outside sliding Mass

acceleration histories for the two-step and single-step procedures, respectively, and Fig. 10 compares the total-displacement histories from the two methods.

The following trends are noted in the results of all time-history analyses (not only those shown here):

The observations made earlier with the sinusoidal excitation remain qualitatively valid. In particular, the differences between the two-step and single-step solutions continue to depend on the proximity to resonance. However, the ratio of permanent displacements calculated by the two approaches is relatively closer to unity for seismic records than sinusoidal excitations.

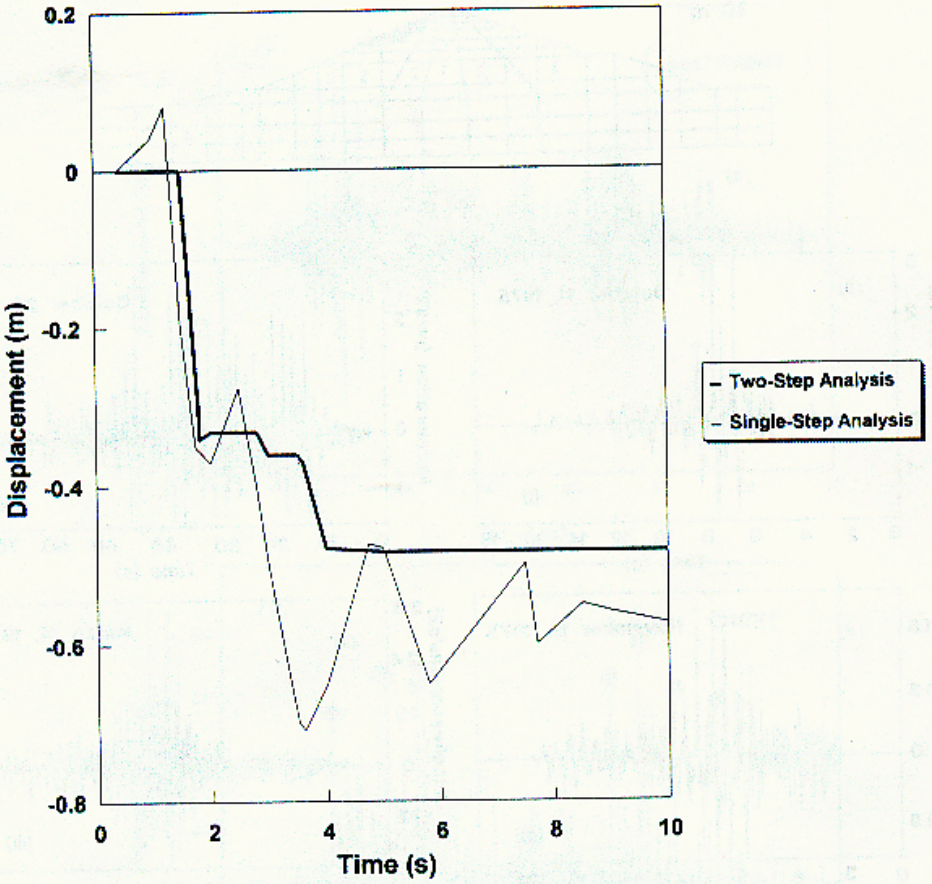

FIG. 10. Comparison of Displacement Histories from Two Methods for Very Strong Excitation (San Salvador 1986, GIC Record)

The two-step method does not always lead to more conservative results as suggested by Lin and Whitman (1983) for the two-mass lumped-parameter model. For example, the permanent displacements of the two-step method for the San Salvador and Imperial Valley excitations are slightly smaller than those of the single-step method (Table 2). It appears that the frequency ratio (ratio of the predominant frequency of the record and the equivalent fundamental period of the dam at the final iteration f/f_1) is 0.3 for the San Salvador record, which is much less than 1; one can explain this result by comparison with the response to sinusoidal motion (Fig. 5). By contrast, for the Coalinga record $f/f_1 \approx 0.70$—a value closer to unity for which Fig. 5 indeed anticipates greater permanent displacements from the two-step method.

The natural frequency of the dam may change if the sliding wedge constitutes a large part of the structure [compare Figs. 8(*a*) and 9(*a*)]. The natural frequency of even the sliding block itself may be excited, resulting in an additional resonance that would appear in the response in the form of high-frequency undulations and spikes, superimposed on the slower oscillations of the complete dam.

CASE HISTORY: EARTHQUAKE RESPONSE OF LA VILLITA DAM

La Villita is a 60-m-high earth-core rockfill dam in Mexico, 13 km upstream from the mouth of the Balsas River. It was constructed in the mid-

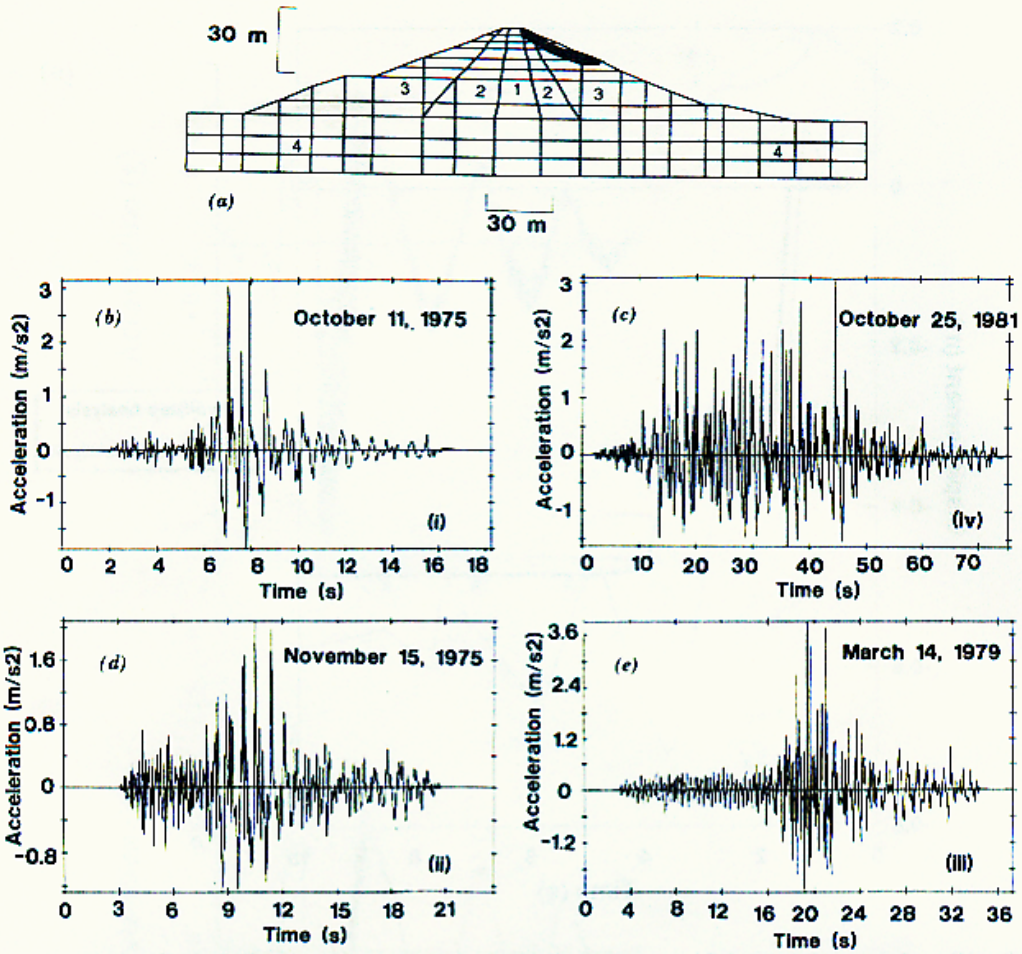

FIG. 11. La Villita Dam Data: (*a*) Finite-Element Discretization with One Sliding Interface (PEPSI); (*b–e*) Accelograms (from Elgamal et al. 1990) Recorded at Dam Crest during Four Earthquake Events

1960s. An alluvial layer of varying thickness (with a maximum of 70 m) lies between the embankment and the bedrock. A finite-element model of the maximum cross section of the dam is shown in Fig. 11(*a*). With slightly curved longitudinal axis and convex upstream, the dam has a clay core and rockfill shells. Cement grouting and a deep cutoff wall control seepage through the alluvium. The dam was instrumented with inclinometers, several rows of benchmarks, and accelerographs, which have furnished the deformation history of the dam since construction ("Performance" 1980).

From 1975–1985, six earthquake events ($4.9 \leq M_L \leq 8.1$) at epicentral distances of 10–120 km subjected the dam to substantial dynamic loads. Five of these earthquakes (the most recent being that of September 19, 1985, which caused extensive damage in Mexico City) contributed to significant measured horizontal and vertical displacements in the dam. Acceleration time histories at the dam crest [Fig. 11(*b–e*)] and nearby free-field bedrock were recorded during these events. As first observed by Elgamal et al. (1990), the transverse crest records observed during the strongest shaking [Figs. 11(*b–e*) and 12(*b*)] display a bias: the negative peaks are consistently smaller than the positive ones. This crest-acceleration bias increases with increasing intensity of shaking. It was attributed to the location of the recording instrument on a section of the dam where localized-type sliding deformation must have taken place (Elgamal et al. 1990). They found

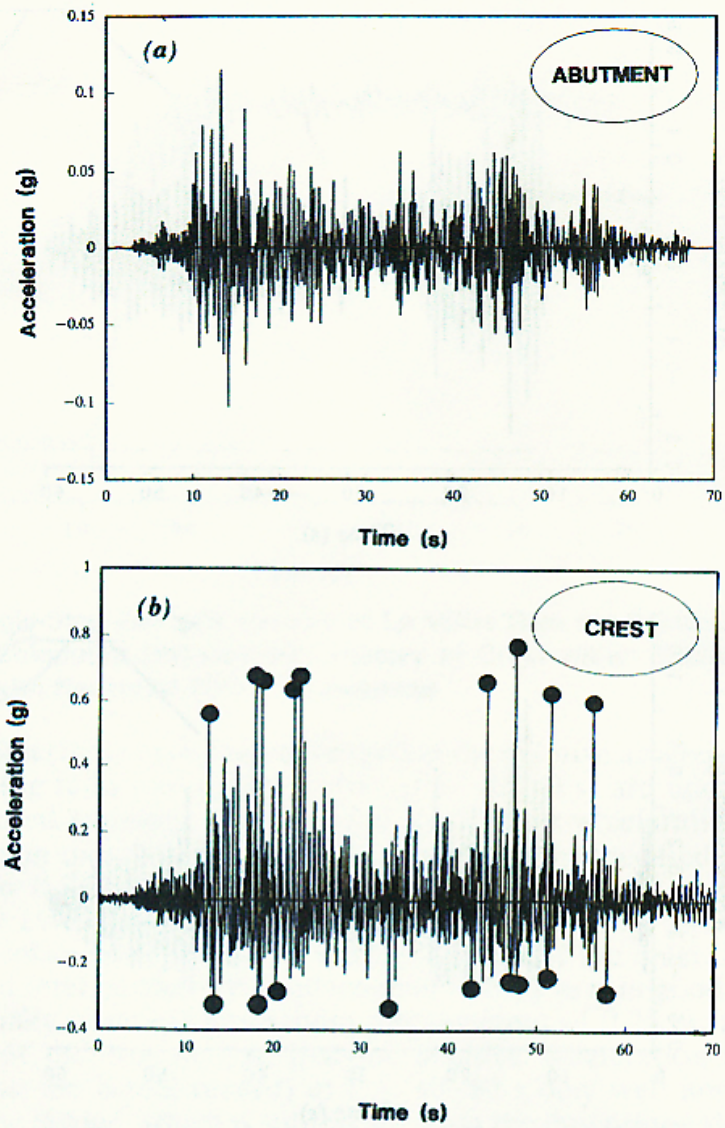

FIG. 12. La Villita Dam Acceleration Histories Recorded during September 19, 1985 Mexico Earthquake (from Elgamal et al.): (*a*) Abutment; and (*b*) Crest

that not only do these records suggest that sliding deformations have taken place, but they also reveal the amplitude of the associated yield (critical) acceleration. For the September 1985 Michoachan event, the crest record displayed in Fig. 12(*b*) shows clearly a yield acceleration of between 0.20 g and 0.30 g.

As a validation of the single-step (PEPSI) procedure proposed, numerical analysis is carried out to explain the observed La Villita dam response at the crest during the Michoachan 1985, $M_s = 8.1$, earthquake. First, a trial-and-error analysis is carried out using a pseudo static slope-stability method to obtain failure surfaces with yield acceleration of 0.25 g. A failure surface beginning at the downstream slope is chosen as a best selection of the sliding surface. Single-step analysis is then performed with this PEPSI to simulate the failure surface, with an assumed friction angle of 38°, based on the available data ("Performance" 1980; Elgamal et al. 1991) and using the geometry of the maximum cross section of the dam [Fig. 11(*a*)]. An average thickness of 35 m is used to represent the underlying alluvial deposit. Three

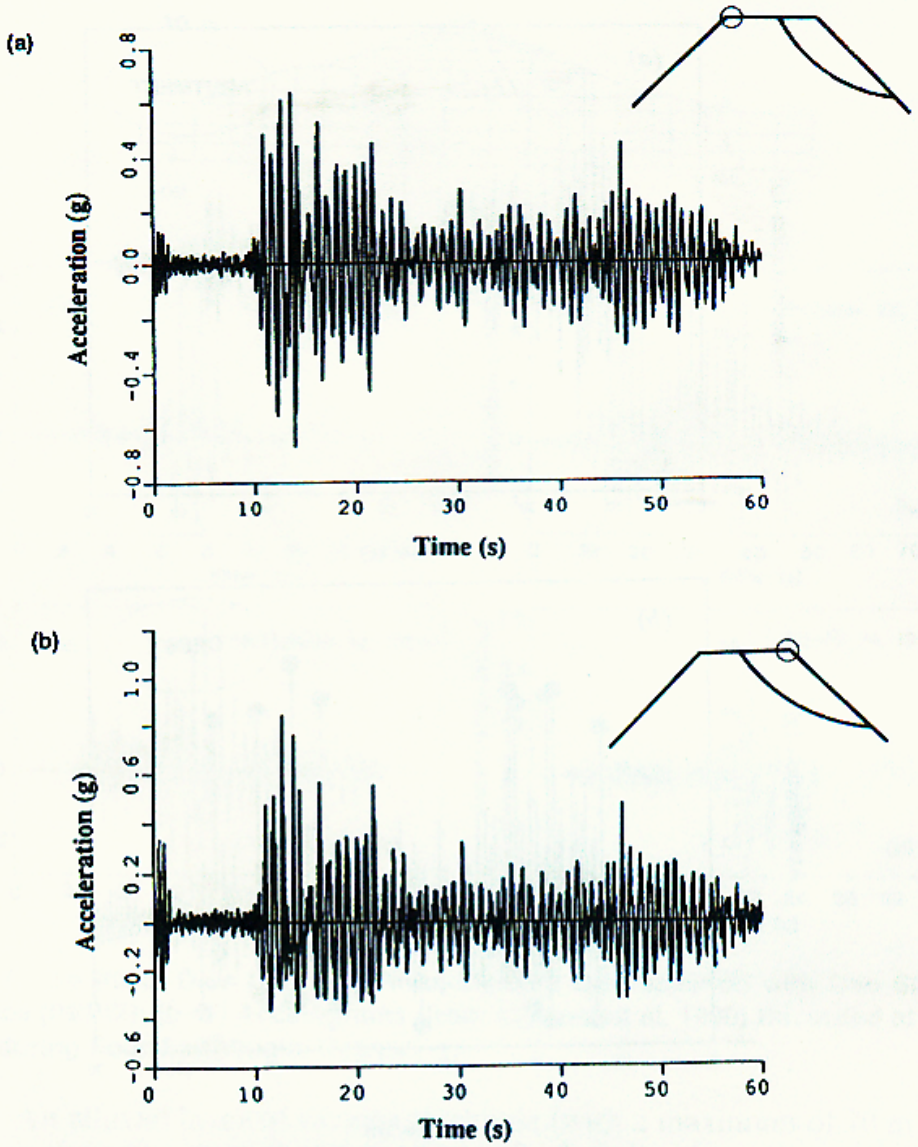

FIG. 13. Single-Step Analysis Results of La Villita Dam for September 19, 1985 Earthquake: (*a*) Crest Acceleration History of a Point Outside Sliding Zone; and (*b*) Crest Acceleration History of a Point within Sliding Zone

materials represent the dam body, and one material represents its alluvial foundation; their properties are from Elgamal et al. (1991).

Iterative two-dimension equivalent linear viscoelastic analyses were performed using ADINA, and produced a fundamental frequency that matched very closely the observed first natural frequency (1.26 Hz) of the dam.

The computed acceleration histories of two points on the crest of the dam, one outside and one inside the sliding block, are plotted in Figs. 13(*a* and *b*). The assymmetry between peak positive and negative values is evident in the acceleration of the "inside" point [Fig. 13(*b*)]. By contrast, the point outside the sliding wedge exhibits a symmetric acceleration history [Fig. 13(*a*)]. Apparently the limited amplitude of the negative peaks can be attributed to the cutting off of these peaks as a consequence of slippage in the downstream direction.

The computed crest-acceleration history within the sliding mass [Fig. 13(*b*)] compares favorably with the observed crest record [Fig. 12(*b*)]. A

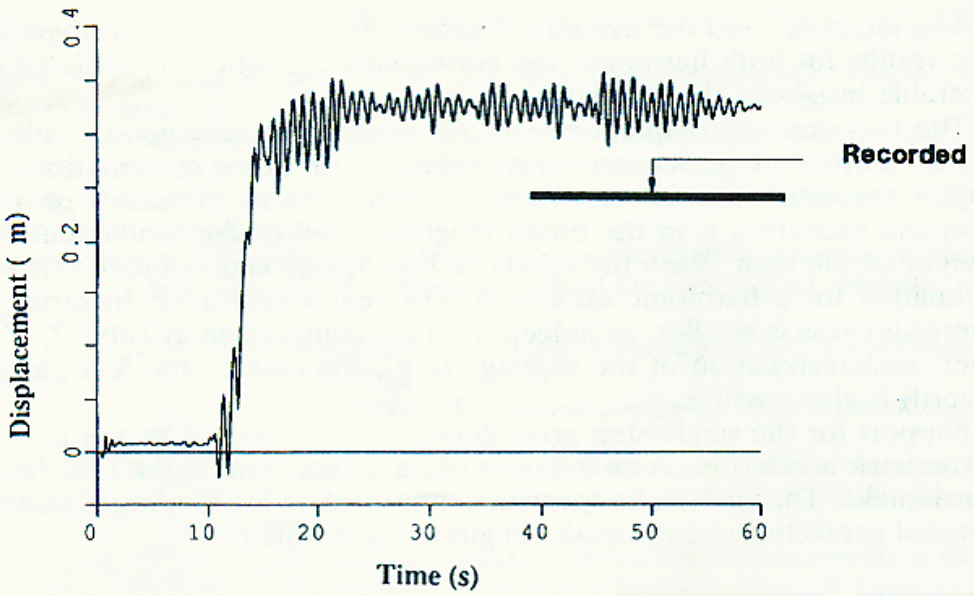

FIG. 14. Single-Step Analysis Results of La Villita Dam for September 19, 1985 Earthquake: Computed Displacement History of Crest within Sliding Zone and Comparison with Recorded Total Displacement

small exception (to be explained later) is that the positive acceleration spikes observed in the later part of the record (t = 40–60 s) are underpredicted in the computed response. As expected, the largest acceleration spikes in the downstream direction only slightly exceed the prespecified yield acceleration, A_y = 0.25 g.

As further evidence of the success of the analysis, Fig. 14 displays the computed displacement history of the sliding part of the crest. Notice that the computed total permanent displacement of 0.32 m is in good agreement with the actually observed permanent displacement of 0.25 m. A plausible explanation of the discrepancy, that the positive acceleration spikes (observed only in the actual record) at t = 40–60 s may well imply upslope slippage of the wedge, which is subtracted from the downslope slippage that occurred earlier at $t \approx$ 12–15 s. In fact, a flatter sliding surface than the one back figured here may in reality have facilitated this upslope slippage, while simultaneously causing larger (instantaneous) accelerations of the wedge than the ones computed here for the steeper sliding surface!

The apparent yield accelerations that emerge from the records of Figs. 11 and 12 increase with increasing intensity of shaking. This is, in our opinion, a result of the strain-hardening (rather than ideally plastic) behavior of the interface after yielding. Thus, only a strong motion, as during the 1985 event, could mobilize the full sliding resistance of the interface. By contrast, the weaker events of 1979 and 1981 induced only partial yielding of elements at the interface.

SUMMARY AND CONCLUSION

Estimation of the permanent deformations of embankment dams in practice is based on the simplifying assumption that dynamic acceleration response and wedge sliding are two separate processes (decoupled elastic and rigid-slip features of dynamic response). An alternative hypothesis was used in the present paper, namely that these two processes occur simultaneously. To this end, the dam was assumed to contain an a priori assigned potentially

sliding interface, and the dynamic response was computed in a single step. The results for both harmonic and earthquake excitations provided a considerable insight to the problem.

The two-step approximation leads, in general, to very good results, although it often provides conservative estimates of sliding deformations. The largest overestimation occurs when the predominant frequency of a narrowband excitation is in the broad neighborhood of the fundamental frequency of the dam. With the charts in Fig. 5, one can estimate this overestimation for a harmonic excitation. For real acceleration histories, the overestimation is smaller, as judged from the comparison in Table 2. Moreover, underestimation of the slippage (e.g., the case of the San Salvador record) is also possible.

Support for the single-step procedure used was offered by the recorded asymmetric accelerogram on the crest of La Villita Dam in the 1985 Mexico Earthquake. The analysis has provided improved understanding of this complicated geotechnical earthquake engineering problem.

APPENDIX. REFERENCES

Ambraseys, N. N. (1973). "Dynamics and response of foundation materials in epicentral regions of strong earthquakes." *5th World Conf. on Earthquake Engrg., Vol. CXXVI*, Rome, Italy.

Ambraseys, N. N., and Sarma, A. K. (1967). "The response of earth dams to strong earthquake." *Géotechnique*, London, England, 17, 181–213.

Bathe, K.-J., and Mijailovich, S. (1988). "Finite element analysis of frictional contact problems." *J. Theoretical and Appl. Mech.*, 7(1), 31–44.

Constantinou, M. C., and Gazetas, G. (1984). "Probabilistic seismic sliding deformations of earth dams and slopes." *Proc., Specialty Conf. on Probabilistic Methods & Structural Reliability*, ASCE, New York, N.Y., 318–321.

Constantinou, M. C., Gazetas, G., and Tadjbakhsh, I. (1984). "Stochastic sliding of rigid mass against asymmetric coulomb friction." *Earthquake Engrg. and Struct. Dynamics*, 12, 777–793.

Dakoulas, P., and Gazetas, G. (1986). "Seismic shear strains and seismic coefficients in dams & embankments." *Soil Dynamics & Earthquake Engrg.*, 5(2), 75–83.

Elgamal, A.-W. M., Scott, R. F., Succarieh, M. F., and Yan, L. (1990). "La Villita Dam response during five earthquakes including permanent deformation." *J. of Geotech. Engrg.*, ASCE, 116(10), 1443–1462.

Gazetas, G. (1981*a*). "Longitudinal vibrations of embankment dams." *J. Geotech. Engrg. Div.*, ASCE, 107(1), 21–40.

Gazetas, G. (1981*b*). "Vertical oscillation of earth and rockfill dams: analysis and field observation." *Soils & Foundations*, 21(4), 265–277.

Hynes-Griffin, M. E., and Franklin, A. G. (1984). "Rationalizing the seismic coefficient methods." *Miscellaneous paper GL-84-13*, U.S. Army Engineer Waterway Experiment Station, Vicksburg, Miss.

Kutter, B. L. (1982). "Centrifugal modeling of the response of clay embankments to earthquakes," PhD thesis, Cambridge University, Cambridge, England.

Lin, J. S., and Whitman, R. V. (1983). "Decoupling approximation to the evaluation of earthquake-induced plastic slip in earth dams." *Earthquake Engrg. and Struct. Dynamics*, 11, 667–678.

Lin, J. S., and Whitman, R. V. (1986). "Earthquake induced displacements of sliding block." *J. Geotech. Engrg.*, ASCE, 105(12), 1427–1434.

Makdisi, F. I., and Seed, H. B. (1978). "Simplified procedure for estimating dam and embankment earthquake-induced deformation." *J. Geotech. Engrg. Div.*, ASCE, 104(7), 849–867.

Makris, N. (1989). "Analysis of harmonically excited sliding systems," MS thesis, State University of New York, Buffalo, N.Y.

Marcuson, W. F. III, Hynes, M. E., and Franklin, A. G. (1992). "Seismic stability and permanent deformation analysis: the last twenty five years." *Proc., ASCE*

Specialty Conf. Stability Perf. of Slopes and Embankments-II, ASCE, New York, N.Y.
Mejia, L. H., Seed, H. B., and Lysmer, J. (1982). "Dynamic analysis of earth dams in three dimensions." *J. Geotech. Engrg. Div.*, ASCE, 108, 1586–1604.
Nadim, F., and Whitman, R. V. (1983). "Seismically induced movements of retaining walls." *J. Geotech. Engrg. Div.*, ASCE, 109(7), 915–931.
Newmark, N. M. (1965). "Effect of earthquakes on dams and embankments." *Géotechnique*, London, England, 15(2), 139–160.
"Performance of El Infiernillo and La Villita dams including the earthquake of March 14, 1979." (1980). *Rep. No. 5*, Comision Federal De Electricidad, Mexico City, Mexico.
Sarma, S. K. (1975). "Seismic stability of earth dam & embankments." *Géotechnique*, London, England, 25(4), 743–761.
Seed, H. B., and Martin, G. R. (1966). "The seismic coefficient in earth dam design." *J. Geotech. Engrg.*, ASCE, 92(3), 25–58.
Seed, H. B., Wong, R. T., Idriss, I. M., and Tokimatsu, K. (1986). "Moduli and damping factors for dynamic analysis of cohesionless soils." *J. Geotech. Engrg.*, ASCE, 112(11) 1016–1032.
Succarieh, M. (1990). "Analysis of earthquake induced large displacements in earth structures," PhD thesis, Rensselaer Polytechnical Institute, Troy, N.Y.
Uddin, N. (1992). "Seismic analysis of earth-core and concrete-face rockfill dams," PhD thesis, State University of New York, Buffalo, N.Y.
Westermo, B., and Udwadia, F. (1983). "Periodic response of a sliding oscillator system to harmonic excitation." *Earthquake Engrg. and Struct. Dynamics*, 11, 135–146.
Yan, L. (1991). "Seismic deformation analysis of earth dams: a simplified method." *Rep. No. SML 91–01*, Soil Mech. Lab., California Institute of Technology, Pasadena, Calif.
Yegian, M. K., and Lahlaf, A. M. (1992). "Dynamic interface shear strength properties of geomembranes and geotextiles." *J. Geotech. Engrg.*, ASCE, 118(5), 760–779.
Yegian, M. K., Marciano E. A., and Ghahraman, V. G. (1991). "Earthquake induced permanent deformations: a probabilistic approach." *J. Geotech. Engrg.*, ASCE, 117(1), 35–50.